Ceramics International 44 (2018) 115–119

Contents lists available at ScienceDirect

Ceramics International

journal homepage: www.elsevier.com/locate/ceramint

Influence of small amounts of gallium oxide addition on ionic conductivity of $La_{0.9}Sr_{0.1}Ga_{0.8}Mg_{0.2}O_{3-\delta}$ solid electrolyte

S.L. Reis*, E.N.S. Muccillo

Energy and Nuclear Research Institute – IPEN, PO Box 11049, S. Paulo 05422-970, SP, Brazil

ARTICLE INFO

Keywords:
A: Powders: solid state reaction
C: Ionic conductivity
D: Perovskites
E: Fuel cells

ABSTRACT

The effects of small amounts of gallium oxide on intragrain and intergrain conductivity of $La_{0.9}Sr_{0.1}Ga_{0.8}Mg_{0.2}O_{3-\delta}$ are investigated by impedance spectroscopy in the 280–420 °C range. Bulk specimens with 0.5, 1.0 and 1.5 mol% gallium oxide are prepared by solid state reaction at 1350 °C. All specimens achieved relative density values higher than 95%. The additive promotes grain growth indicating solid solution formation. A small fraction of the additive remains at grain boundaries and increases the fraction of the gallium-rich, $LaSrGa_3O_7$, impurity phase. The intragrain conductivity of gallium oxide containing specimens is higher than that of the parent solid electrolyte. Similar effect is found for the intergrain conductivity, which is maximum for 1 mol% gallium oxide addition.

1. Introduction

Sr- and Mg-doped lanthanum gallate constitutes a family of oxide-ion conductors with wide electrolytic domain and low electronic conductivity in a wide range of oxygen partial pressures [1,2]. These solid electrolytes have been intensively investigated for application in electrochemical devices such as solid oxide fuel cells [1–3]. One of the main concerns related to these oxide-ion conductors are the frequently detected impurity phases ($LaSrGaO_4$, $LaSrGa_3O_7$, $La_4Ga_2O_9$ and free MgO), which are believed to be consequence of gallium loss during high temperature heat treatments, besides the complex reactions among the several constituents [4,5].

Doped lanthanum gallates are more often prepared by the cost-effective conventional method of mixing the starting reagents followed by high temperature reaction, which is generally accompanied by introduction of some additives to facilitate the processing steps. Metal oxides are usually added during processing of polycrystalline ceramics for several purposes, such as sintering aid, grain growth control, phase stabilization or to favor a specific property (optical, thermal, mechanical or electrical). Relatively few studies may be found concerning the introduction of additives in the processing of lanthanum gallates, in contrast to other oxide-ion conductors (see for example [6,7]).

Ishihara et al. [8] reported the effect of transition metal oxide additions to the electrical properties of $La_{0.8}Sr_{0.2}Ga_{0.8}Mg_{0.2}O_{3-\delta}$. Introduction of Fe in the Ga site promoted stabilization of the cubic perovskite structure and increase of the solubility of Sr in the La site, although the transference number decreased accordingly. These transition metal oxides were found to increase both the ionic and the electronic conductivity. Ha et al. [9] investigated the effects of manganese oxide and other additives including transition metal and multivalent oxides in $La_{0.8}Sr_{0.2}Ga_{0.8}Mg_{0.2}O_{3-\delta}$. Improved densification, phase purity and electrical conductivity for V, Zn, Si, Co and Fe additions, whereas B, Bi, Li and Si deterioration of the grain boundary conductivity were reported.

The effect of excess-Mg on the microstructure and electrical conductivity of $La_{0.8}Sr_{0.2}Ga_{0.83}Mg_{0.17+x}O_{3-\delta}$ was reported to produce enrichment of grain boundaries with a Mg-rich second phase [10] and increased electrical conductivity.

The influence of depleted and excess gallium concentrations in $La_{0.8}Sr_{0.2}Ga_{0.8}Mg_{0.2}O_{3-\delta}$ was studied by Ahmad-Khanlou et al. [11]; differences in phase contents, sintering behavior and electrical conductivity were found for both hypo- and hyperstoichiometric compositions. The activation energy for conduction increased with increasing Ga content.

In these studies the base compositions were those with cubic perovskite structure, probably because they display the highest ionic conductivity values among the oxide-ion conductors within the lanthanum gallate family. However, compositions with that structure also possess the highest fraction of impurity phases [12]. In addition, the sintering temperature in these studies was higher than 1400 °C, the melting point of the $LaSrGaO_4$ impurity phase that is known to influence the sintering process [11]. These interfering effects might have obscured the possible influence of excess gallium to compensate for its loss during sintering.

* Correspondence to: Center of Materials Science and Technology, Energy and Nuclear Research Institute – IPEN, PO Box 11049, S. Paulo 05422-970, SP, Brazil.
E-mail address: shirley.reis@usp.br (S.L. Reis).

http://dx.doi.org/10.1016/j.ceramint.2017.09.139
Received 14 July 2017; Received in revised form 16 September 2017; Accepted 18 September 2017
Available online 20 September 2017

In this work the effects of small amounts of gallium oxide on sintering, phase composition and ionic conductivity of $La_{0.9}Sr_{0.1}Ga_{0.8}Mg_{0.2}O_{3-\delta}$ prepared by the conventional solid state reaction were investigated. The processing steps were optimized in order to produce to dense specimens sintered at lower temperatures than usual [13] to minimize Ga loss from the starting composition.

2. Experimental procedure

2.1. Materials and preparation method

$La_{0.9}Sr_{0.1}Ga_{0.8}Mg_{0.2}O_{3-\delta}$ nominal composition, hereafter LSGM, was prepared by the solid state reaction method with La_2O_3 (99.9%), Ga_2O_3 (99.99%), $SrCO_3$ (P.A.) and MgO (P.A.) as precursor materials. First, the lanthanum oxide precursor was heat treated at 1000 °C for 3 h. Afterwards, stoichiometric amounts of the starting materials were weighted and thoroughly mixed. The mixed powder was thermally treated at 1250 °C for 4 h and deagglomerated in an agate mortar with pestle. This procedure was repeated twice. Finally, the powder was attrition milled in isopropyl alcohol with zirconia balls (ϕ 2 mm) for 1 h, and dried in an oven. These processing steps have been successfully employed by the authors to prepare dense specimens [13,14].

Small amounts (0.5, 1.0 and 1.5 mol%) of Ga_2O_3 were added to the thermally treated powder mixture, homogenized in acetone and dried.

Cylindrical specimens were prepared by uniaxial and cold isostatic pressing (200 MPa). Green compacts were sintered (Lindberg BlueM) at 1350 °C for 5 h with 5 and 10 °C min^{-1} heating and cooling rates, respectively. The sintering temperature was selected taking into account the well-known loss of gallium at high temperatures.

2.2. Characterization methods

The crystalline structure of the powder mixtures as well as sintered specimens was analized by X-ray diffraction, XRD (Bruker-AXS, D8 Advance) in the 20–80° 2θ range with Ni-filtered Cu Kα radiation (λ = 1.5405 Å), 0.05° step size and 2 s time per step. Indexing of diffraction peaks was carried out by comparison of the experimental patterns with the PDF 70-2787 of the orthorhombic perovskite phase of LSGM. The collected diffraction patterns were normalized by the highest intensity peak of the orthorhombic phase for comparison purposes. Impurity phases were identified according to the following PDF files: 74-1610 (Ga_2O_3), 37-1433 ($La_4Ga_2O_9$), 24-1208 ($LaSrGaO_4$) and 45-0637 ($LaSrGa_3O_7$). The apparent density of sintered specimens was determined by the water immersion method. Relative density values were evaluated taken into account the theoretical density (6.67 g cm^{-3}, PDF 70-2787) of the orthorhombic phase of LSGM. The mean grain size, G, was estimated by the intercept method [15] from micrographs obtained by field emission gun scanning electron microscopy, FEG-SEM (FEI, Inspect F50) on polished and thermally etched surfaces of sintered specimens.

The ionic conductivity was determined by impedance spectroscopy (Hewlett Packard 4192A) in the 5 Hz to 13 MHz frequency range, with 100 mV applied signal. The impedance spectrum was collected during heating up the specimens from 280 to 420 °C. Silver paste was applied by painting onto surfaces of specimens followed by heat treatment at 400 °C to act as electrode material. The impedance data were analyzed by special software [16].

3. Results and discussion

3.1. Structure, density and microstructure

Fig. 1 shows XRD patterns of calcined powder mixtures. Diffraction peaks indicated by * correspond to those of $La_{0.9}Sr_{0.1}Ga_{0.8}Mg_{0.2}O_{3-\delta}$ with orthorhombic structure. After calcination at 1250 °C the $La_4Ga_2O_9$ (PDF 37-1433) impurity phase (indicated by # 2) has already been formed. In addition, small-intensity peaks of unreacted Ga_2O_3 (PDF 74-1610) are recorded in all these patterns, evidencing that higher temperatures should be used for reaction completion.

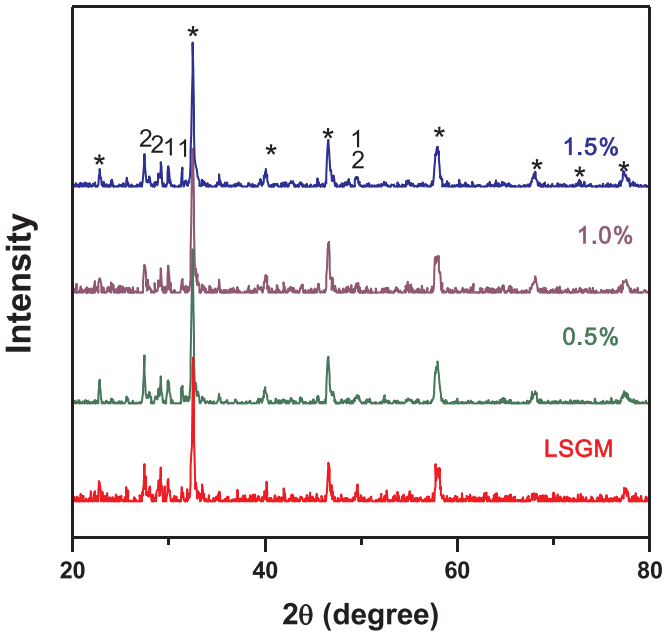

Fig. 1. Room temperature XRD patterns of powder mixtures of LSGM with and without gallium oxide addition. (*) LSGM orthorhombic phase, (1) Ga_2O_3 and (2) $La_4Ga_2O_9$.

The XRD patterns of sintered LSGM specimens with and without gallium oxide addition are depicted in Fig. 2a. The Miller indexes of the orthorhombic structure also are shown. These patterns reveal that all sintered specimens are primarily constituted by the characteristic orthorhombic perovskite-like phase. Low-intensity diffraction peaks are due to common impurity phases (Fig. 2b), except that in 2θ ~ 38°, which is due to β-Ga_2O_3 (PDF 74-1776) with monoclinic structure.

Fig. 2b highlights the 25–32° 2θ angular range, where most of the high-intensity diffraction peaks of impurity phases are detected. The XRD pattern of LSGM sintered at 1350 °C for 5 h exhibits the characteristic peak (2θ ~ 31.4°) of $LaSaGaO_4$ (PDF 24-1208) as the main impurity phase. Specimens containing gallium oxide, in contrast, show the diffraction peak (2θ ~ 30°) of the rich-gallium ($LaSrGa_3O_7$, PDF 45-0637) impurity phase. Traces of the $La_4Ga_2O_9$ phase are observed in all patterns. These results suggest that at least a fraction of gallium oxide added to LSGM do not enter into solid solution with LSGM, and is used to form the rich-gallium phase at expenses of other impurity phases. Nevertheless, the total amount of impurity phases decreased with increasing Ga_2O_3 content.

Sintering at 1350 °C allowed for obtaining dense LSGM specimens. Table 1 lists values of relative density for the several studied compositions. The relative density was evaluated neglecting the density of gallium oxide (6.47 g cm^{-3}, PDF 74-1610), which is slightly lower than that of LSGM and because of the relative small amounts of Ga_2O_3 added to the base material. In addition, the fraction of impurity phases is also small and neglected in this calculation. Relative density values obtained for all specimens are higher than 95% evidencing the high sinterability of the powders.

The main microstructure features of LSGM (Fig. 3a) consist of polygonal grains with mean size in the micrometer range and residual porosity at grain boundaries. The same characteristic features hold for specimens containing gallium oxide. Fig. 3b shows, as example, a FEG-SEM micrograph of LSGM containing 1.5 mol% Ga_2O_3.

Table 1 summarizes the mean grain size values of sintered specimens. The grain size increases slightly with gallium oxide addition, such that about 6% increase of G occurs for 1 mol% addition. This effect

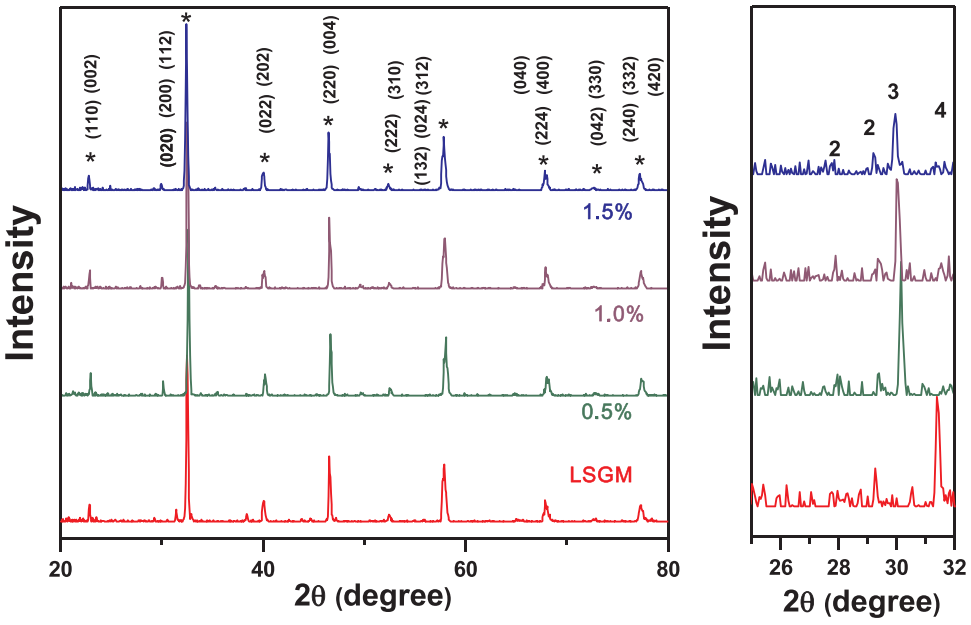

Fig. 2. Room temperature XRD patterns of sintered LSGM specimens with and without gallium oxide addition in the (a) 20–80° and (b) 25–32° 2θ ranges. Miller indexes of PDF 70-2787 file of the LSGM orthorhombic phase, (2) $La_4Ga_2O_9$, (3) $LaSrGa_3O_7$, and (4) $LaSrGaO_4$.

Table 1
Values of relative density (%) and mean grain size, G (μm), of sintered LSGM specimens with and without gallium oxide addition.

Ga_2O_3 (mol%)	Relative density (%)	G (μm)
–	98.5	2.30 ± 0.07
0.5	96.7	2.95 ± 0.08
1.0	95.2	3.13 ± 0.09
1.5	95.0	3.16 ± 0.08

is probably associated to the reduction in the fraction of impurity phases, which might inhibit grain growth. In other words, addition of Ga_2O_3 to LSGM promoted grain growth. These results reveal that a fraction of the additive forms solid solution with LSGM during sintering. Similar effect was observed previously in doped ceria ion-conductors [17,18].

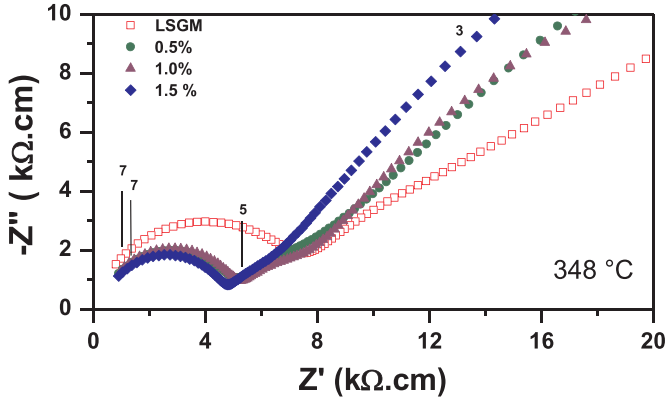

Fig. 4. Impedance spectroscopy diagrams of LSGM with and without gallium oxide addition recorded at 348 °C. Numbers over experimental data stand for logarithm of frequency (in Hz).

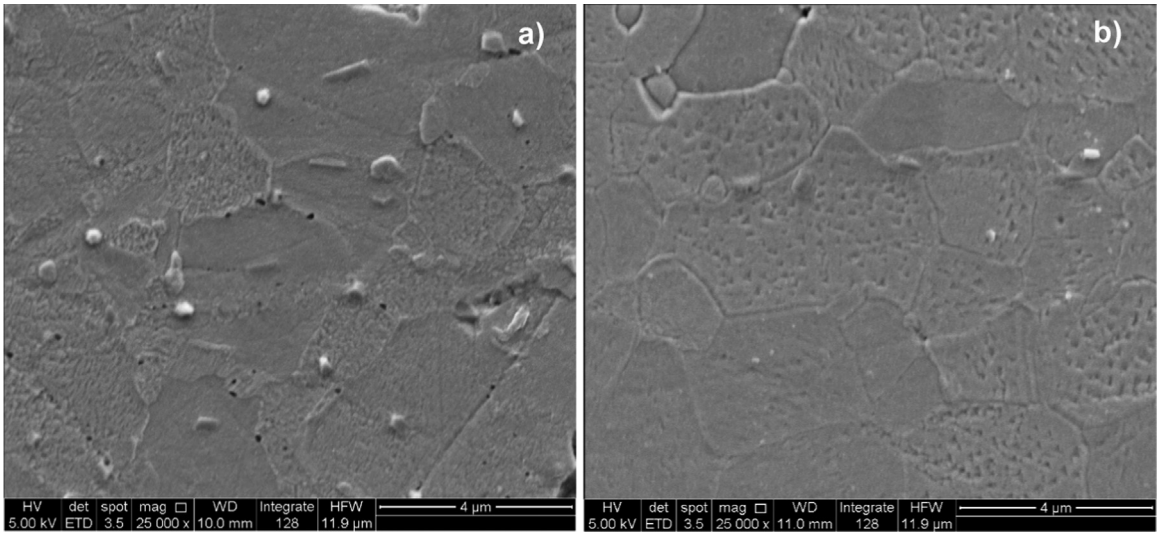

Fig. 3. FEG-SEM images of (a) LSGM and (b) LSGM containing 1.5 mol% gallium oxide specimens sintered at 1350 °C.

Table 2
Values of intra- and intergrain capacitance, and total activation energy for conduction of LSGM specimens with and without gallium oxide addition.

Ga_2O_3 (mol%)	E_T (eV)	C_g (10^{-11} F)	C_{ig} (10^{-9} F)
–	1.16 ± 0.05	1.15	1.64
0.5	0.98 ± 0.05	1.34	2.78
1.0	0.96 ± 0.05	1.16	2.25
1.5	1.00 ± 0.05	1.21	3.75

3.2. Ionic conductivity

The ionic conductivity of LSGM with and without gallium oxide addition was determined by impedance spectroscopy in a temperature range such that the intragrain and intergrain components may be evaluated. Fig. 4 shows [− Z″(ω) × Z′(ω)] diagrams recorded at approximately 350 °C. Numbers over experimental points are the logarithm of the frequency. The impedance spectroscopy spectra were normalized for specimen dimensions.

The high-frequency arc is assigned to resistive and capacitive effects of the bulk (or intragrain). The capacitance (C_g) value estimated in the apex of the arc (Table 2) is about 1.10^{-11} F. The intermediate-frequency arc arises primarily from the combined effect of impurity phases, which show low-conductivity [5] and residual porosity at interfaces. Nevertheless, the comparatively low intensity of the intermediate-frequency arc reveals that the consequent blocking effect exerts minor influence on the overall ionic conductivity. Typical capacitance values for the intermediate-frequency arc (C_{ig}) are in the nanoFarad range (Table 2). The electrode arc at low-frequencies reflects the interactions at the interface between LSGM and electrode and was not analyzed.

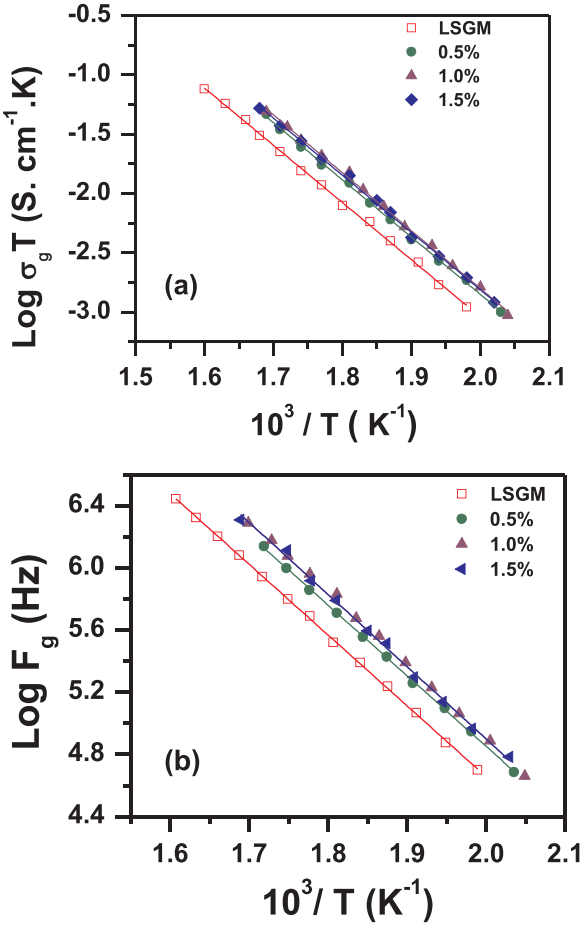

Fig. 5. Arrhenius plots of the intragrain (a) conductivity and (b) relaxation frequency of LSGM specimens with and without gallium oxide addition.

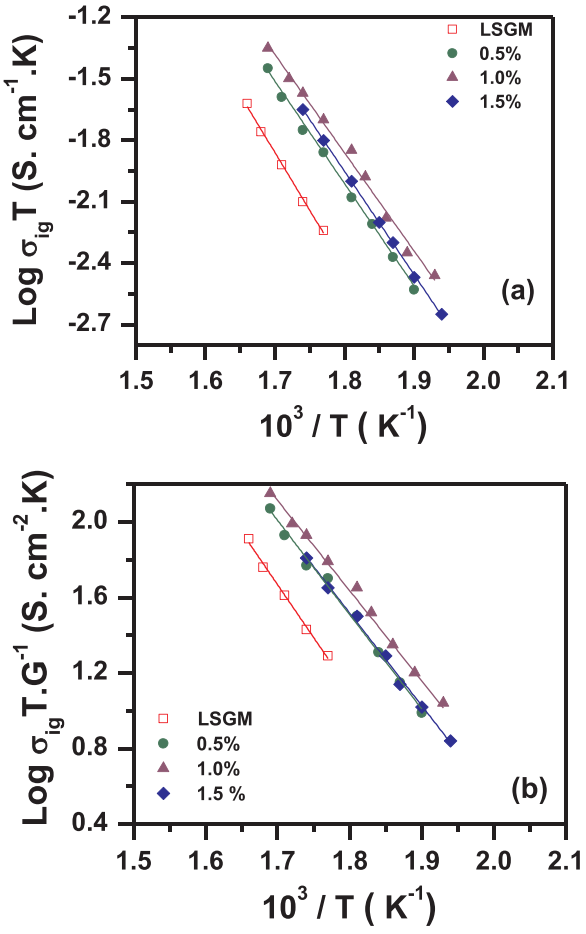

Fig. 6. Arrhenius plots of the intergrain conductivity of LSGM specimens with and without gallium oxide addition (a) before and (b) after normalization by the mean grain size.

Arrhenius plots of the intragrain conductivity, σ_g, are shown in Fig. 5a. Parallel straight lines were obtained for the studied compositions evidencing no change in the overall conduction mechanism. It is worth noting the high intragrain conductivities of LSGM specimens containing gallium oxide. This result is a further evidence that a fraction of the added Ga_2O_3 forms solid solution, probably as a compensation effect due to possible gallium loss during sintering.

Fig. 5b depicts the logarithm of the relaxation frequencies determined in the apex of the intragrain arc as function of reciprocal temperature. The relaxation frequency increases with gallium oxide additions evidencing differences in the bulk characteristics of specimens with and without gallium oxide.

Fig. 6 shows the Arrhenius plots of the intergrain conductivity of LSGM specimens with and without gallium oxide addition (a) before and (b) after normalization for the mean grain size. The LSGM specimen without Ga_2O_3 addition exhibits (Figs. 6a and 6b) the lowest intergrain conductivity. This effect reveals that addition of small amounts of gallium oxide to LSGM has a beneficial effect also at the grain boundaries, even with increasing the fraction of the insulating rich-gallium phase [11]. Values of the total activation energy for conduction are listed in Table 2. It may be noted a net tendency to decrease the activation energy value up to 1.0 mol% Ga_2O_3, although those values are within the experimental uncertainties. The highest intergrain conductivity is found for LSGM containing 1.0 mol% Ga_2O_3 and corresponds to an increase of about half-order of magnitude to that of LSGM without the additive. Therefore, small amounts of gallium oxide optimize the overall ionic conductivity of LSGM.

4. Conclusions

Small amounts of gallium oxide was added to $La_{0.9}Sr_{0.1}Ga_{0.8}Mg_{0.2}O_{3-\delta}$ by solid state synthesis. Solid solution between both components was evidenced by increase of the ionic conductivity, whereas X-ray diffraction revealed formation of the rich-gallium phase ($LaSrGa_3O_7$) at the expenses of other impurity phases. The addition of gallium oxide promoted grain growth and reduction of the relative fraction of impurity phases. The intragrain and intergrain components of the total ionic conductivity increased up to 1.0 mol% gallium oxide addition to LSGM revealing the enhancement of the electrical properties of doped lanthanum gallate.

Acknowledgements

The authors acknowledge FAPESP (Procs. 96/09604-9 and 2013/07296-2), CNPq (Proc. 304073/2014-8) and CNEN for financial support. One of the authors (S.L.Reis) acknowledges CNPq (Proc. 505980/2013-4) for the scholarship.

References

[1] T. Ishihara, M. Honda, Y. Takita, Doped $LaGaO_3$ perovskite type oxide as a new oxide ionic conductor, J. Am. Chem. Soc. 116 (1994) 3801–3803.
[2] M. Feng, J.B. Goodenough, A superior oxide-ion electrolyte, Eur. J. Solid State Inorg. Chem. 31 (1994) 663–672.
[3] T. Ishihara, Low temperature solid oxide fuel cells using $LaGaO_3$-based oxide electrolyte on metal support, J. Jpn. Pet. Inst. 58 (2015) 71–78.
[4] J.W. Stevenson, T.R. Armstrong, I.R. Pederson, J. Li, C.A. Levinson, S. Baskaran, Effect of A-site cation nonstoichiometry on the properties of doped lanthanum gallate, Solid State Ion. 113–115 (1998) 571–583.
[5] M. Rozumek, P. Majewski, F. Aldinger, K. Künstler, G. Tomandl, Preparation and electrical conductivity of common impurity phases in $(La,Sr)(Ga,Mg)O_3$ solid electrolytes, CFI-Ber. DKG 80 (2003) E35–E40.
[6] J.D. Nicholas, L.C. De Jonghe, Prediction and evaluation of sintering aids for cerium gadolinium oxide, Solid State Ion. 178 (2007) 1187–1194.
[7] A.J. Fleger, T.E. Burye, Q. Yang, J.D. Nicholas, Cubic yttria stabilized zirconia sintering additive impacts: a comparative study, Ceram. Int. 40 (2014) 16323–16335.
[8] T. Ishihara, H. Furutani, T. Yamada, Y. Takita, Oxide ion conductivity in double doped lanthanum gallate perovskite type oxide, Ionics 3 (1997) 209–213.
[9] S.B. Ha, Y.H. Cho, Y.C. Kang, J.-H. Lee, J.-H. Lee, Effect of oxide additives on the sintering behavior and electrical conductivity of strontium- and magnesium-doped lanthanum gallate, J. Eur. Ceram. Soc. 30 (2010) 2593–2601.
[10] X. Zhao, X. Li, N. Xu, K. Huang, Beneficial effects of Mg-excess in $La_{1-x}Sr_xGa_{1-y}Mg_{y+z}O_{3-\delta}$ as solid electrolyte, Solid State Ion. 214 (2012) 56–61.
[11] A. Ahmad-Khanlou, F. Tietz, D. Stöver, Material properties of $La_{0.8}Sr_{0.2}Ga_{0.9+x}Mg_{0.1}O_{3-\delta}$ as a function of Ga content, Solid State Ion. 135 (2000) 543–547.
[12] P. Datta, P. Majewski, F. Aldinger, Synthesis and microstructural characterization of Sr- and Mg-substituted $LaGaO_3$ solid electrolyte, Mater. Chem. Phys. 102 (2007) 240–244.
[13] S.L. Reis, E.N.S. Muccillo, Preparation of dense $La_{0.9}Sr_{0.1}Ga_{0.8}Mg_{0.2}O_{3-\delta}$ by solid state synthesis, Ion. (2017) (Submitted for publication).
[14] S.L. Reis, E.N.S. Muccillo, Microstructure and electrical conductivity of fast fired Sr- and Mg-doped lanthanum gallate, Ceram. Int. 42 (2016) 7270–7277.
[15] M.J. Mendelson, Average grain size in polycrystalline ceramics, J. Am. Ceram. Soc. 52 (1969) 443–446.
[16] M. Kleitz, J.H. Kennedy, P. Vashishta, J.N. Mundy, G.K. Shenoy (Eds.), Fast Ion Transport in Solids, Electrodes and Electrolytes, North-Holland, Amsterdam, 1979, pp. 185–186.
[17] H. Yoshida, K. Miura, J.-I. Fujita, T. Inagaki, Effect of gallia addition on the sintering behavior of samaria-doped ceria, J. Am. Ceram. Soc. 82 (1999) 219–221.
[18] S.-W. Seo, J.-H. Park, M.-W. Park, J.-H. Koo, K.-T. Lee, J.-S. Lee, Effects of gallia addition on the sintering behavior and electrical conductivity of yttria-doped ceria, Electron. Mater. Lett. 10 (2014) 791–794.